



Article

Modeling and Predicting the Mechanical Behavior of Standard Insulating Kraft Paper Used in Power Transformers under Thermal Aging

Ahmed Sayadi ^{1,2}, Djillali Mahi ¹, Issouf Fofana ^{3,*} , Lakhdar Bessissa ⁴, Sid Ahmed Bessedik ⁵, Oscar Henry Arroyo-Fernandez ⁶ and Jocelyn Jalbert ⁶ 

¹ Laboratory of Studies and Development of Semiconductor and Dielectric Materials, LeDMaScD, University Amar Telidji of Laghouat, BP 37G Route of Ghardaïa, Laghouat 03000, Algeria; a.sayadi@ens-lagh.dz (A.S.); d.mahi@lagh-univ.dz (D.M.)

² Laboratory of Applied and Didactic Sciences, Higher Normal School of Laghouat, BP 4033, Laghouat 03000, Algeria

³ Research Chair on the Aging of Power Network Infrastructure (ViaHT), University of Québec, Saguenay, QC G7H 2B1, Canada

⁴ Materials Science and Informatics Laboratory (MSIL), University Ziane Achour of Djelfa, BP 3117 Route of Moudjbara, Djelfa 17000, Algeria; lakhdarbessissa@gmail.com

⁵ Laboratory for Analysis and Control of Energy Systems and Electrical Systems (LACOSERE), Laghouat University, Laghouat 03000, Algeria; s.bessedik@lagh-univ.dz

⁶ Research Institute d'Hydro-Québec, 1800 Boulevard Lionel-Boulet, Varennes, QC J3X 1S1, Canada; arroyo.oscar@ireq.ca (O.H.A.-F.); jalbert.jocelyn@ireq.ca (J.J.)

* Correspondence: ifofana@uqac.ca

Abstract: The aim of this research is to predict the mechanical properties along with the behaviors of standard insulating paper used in power transformers under thermal aging. This is conducted by applying an artificial neural network (ANN) trained with a multiple regression model and a particle swarm optimization (MR-PSO) model. The aging of the paper insulation is monitored directly by the tensile strength and the degree of polymerization of the solid insulation and indirectly by chemical markers using 2-furfuraldehyde compound content in oil (2-FAL). A mathematical model is then developed to simulate the mechanical properties (degree of polymerization (DP_V) and tensile index ($Tidx$)) of the aged insulation paper. First, the datasets obtained from experimental results are used to create the MR model, and then the optimizer method PSO is used to optimize its coefficients in order to improve the MR model. Then, an ANN method is trained using the MR-PSO to create a nonlinear correlation between the DP_V and the time, temperature, and 2-FAL values. The acquired results are assessed and compared with the experimental data. The model presents almost the same behavior. In particular, it has the capability to accurately simulate the nonlinear property behavior of insulation under thermal aging with an acceptable margin of error. Since the life expectancy of power transformers is directly related to that of the insulating paper, the proposed model can be useful to maintenance planners.

Keywords: modeling; prediction; mechanical behavior; particle swarm optimization; neural networks; power transformers



Citation: Sayadi, A.; Mahi, D.; Fofana, I.; Bessissa, L.; Bessedik, S.A.; Arroyo-Fernandez, O.H.; Jalbert, J. Modeling and Predicting the Mechanical Behavior of Standard Insulating Kraft Paper Used in Power Transformers under Thermal Aging. *Energies* **2023**, *16*, 6455. <https://doi.org/10.3390/en16186455>

Academic Editors: Frede Blaabjerg and Pawel Rozga

Received: 12 April 2023

Revised: 25 August 2023

Accepted: 27 August 2023

Published: 6 September 2023



Copyright: © 2023 by the authors. Licensee MDPI, Basel, Switzerland. This article is an open access article distributed under the terms and conditions of the Creative Commons Attribution (CC BY) license (<https://creativecommons.org/licenses/by/4.0/>).

1. Introduction

At present, guaranteeing consumers safe and available energy in the best conditions is the major concern of all producers and distributors of electrical energy. Any outage in the distribution of energy always leads to extremely costly consequences. Among the essential equipment in electrical networks are power transformers. They play an important role in the supply of electrical energy, from production to distribution, to consumers. Any unpredictable outage or shutdown of these important machines can cause damage to

the electrical networks and lead to significant financial losses. Their reliability is of such importance that they require special attention.

The general concept of large power transformers, as well as their materials and components, remain practically unchanged compared to the first versions, even with the continued advancement of digitalization. Most power transformers have been using the same insulating materials, paper and oil, in transformer windings for at least 100 years [1]. The ideal scenario is for the physical and chemical qualities to remain unaltered during the transformers' useful lives. Unfortunately, this is not possible in real life because, in practical applications, insulation systems are subjected to several types of stresses: electrical, thermal, mechanical, and environmental origins.

These stresses give rise to internal faults that develop slowly, leading to the progressive deterioration of the insulation. Faults, initially intermittent, then begin to persist in the system. If they are not detected on time and corrected, they can lead to catastrophic failures and consequently generate high financial losses. Any paper impregnated with an insulating fluid ages and gradually loses its original characteristics. Concerning the mechanical and dielectric properties, these are the two main properties that paper must maintain in the life cycle of power transformers. In fact, the dielectric properties of the paper remain almost unchanged in all phases of cellulose aging and do not promote the failure of transformers [2,3]. Under service conditions, the mechanical performance of the paper is altered due to the depolymerization of the cellulose chains, thus leading to a weakened material.

The development of reliable and accurate models is necessary to estimate and predict the progression of degradation and residual life of power transformers. Such models may allow researchers, scientists, and engineers to efficiently use the database and to determine, with greater accuracy and speed, the future state of the insulation system.

In recent years, new techniques, such as fuzzy inference systems (FLs) and ANN, have been applied to develop predictive models for the purpose of estimating the required parameters. These techniques are widely used and have been employed by many researchers for various engineering works [4–12].

The goal of this paper is to model and predict the mechanical properties of insulation using a method based on the analysis of a multiple regression model (MR) optimized by a particle swarm optimization (PSO) algorithm. In the second step, the same optimized model is implemented in an ANN to more accurately predict the behavior of the mechanical properties of the insulating paper samples that undergo accelerated thermal stress aging.

Our study aims to develop a prediction model for the mechanical behavior of standard insulating kraft paper used in power transformers under thermal aging conditions. The degradation of insulating materials can have significant implications for the performance and safety of power transformers, making this an important area of research. To the best of our knowledge, there have been previous studies on the degradation of insulating materials under various aging conditions. However, our study is novel in its approach to developing a prediction model for the mechanical behavior of Kraft paper specifically under thermal aging conditions. This can potentially contribute to the development of more effective strategies for predicting the long-term behavior of power transformers and ensuring their safe and reliable operation.

2. Experimental Procedures

In this work, it is important to point out that the database was used to test the intelligent system. The results of the experiments can be found in [13]. Measurements were performed on kraft paper impregnated in Luminol oil under the influence of different levels of applied temperature (150 °C, 170 °C, and 190 °C), as seen the Appendix A of the paper [13,14].

The experimental data related to the loss of the mechanical properties of different types of cellulosic papers impregnated with insulating liquids during accelerated thermal aging in order to study the DP_V of cellulose and the mechanical properties of the papers.

In this study, standard kraft paper was impregnated with Luminol mineral oil according to American Standard for Testing and Materials (ASTM D-2413). The steps followed for the acquisition of the results are described as follows: [13].

2.1. Materials

The aging cells were used to simulate the environment of a power transformer. Inside each cell were placed the main materials contained in real power transformers: a sample holder composed of copper, paper, and insulating fluid. The aging cell and its contents were sealed in an ambient atmosphere.

Before the paper and fluid were introduced into the aging cells, they were conditioned to equilibrium in dry air with a relative humidity of 0.9% RH inside a double glove box at 20.8 °C.

For a period of 48 h, the holders containing the paper strips were kept in a double glove box's antechamber under vacuum at 40 °C. In this first step of drying, the initial relative humidity (RH) of the paper was decreased from more than 1% RH to less than 0.5% RH. The paper samples were then transferred from the antechamber to the glove box.

The paper samples were conditioned there for at least a week to obtain the nominal RH of 0.9%. Before the aging tests began, the ultimate absolute water content was determined using a coulometric Karl Fisher titration in accordance with ASTM D3277.

The paper samples (13 samples per support) were placed between the windings to avoid contact between the papers and to allow free circulation of the insulating fluid between them. The samples were then placed in the test cell before impregnation (Figure 1).

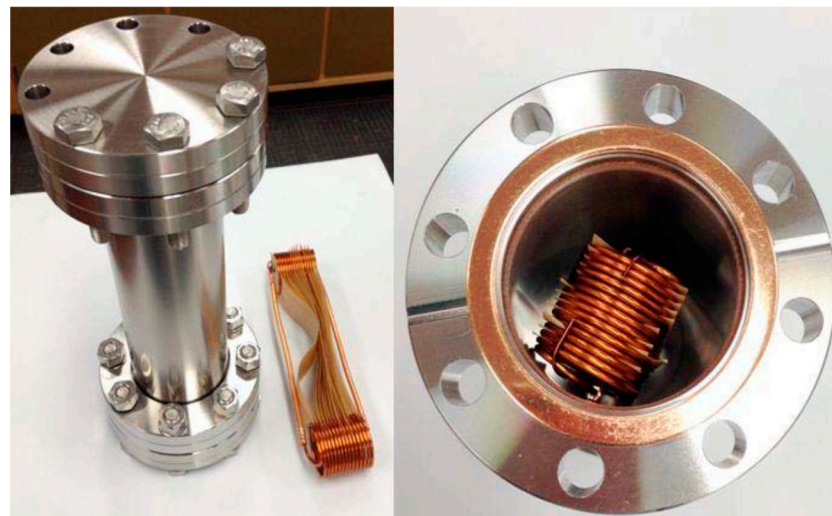


Figure 1. Sample racks and arrangement of the paper samples between the turns of the coil inserted in the aging cell [13].

Then, an oven with forced air was used to house the stainless-steel aging cells (Salvis Lab, type TC-100, Québec, QC, Canada), as shown in Figure 2. The thermal aging was conducted at 150, 170, and 190 °C, respectively, in order to obtain different aged samples in a reasonable time.



Figure 2. Aging cells placed inside an oven with forced air [13].

2.2. Analysis Techniques

Using high-performance liquid chromatography (Agilent, 1100 series PLC, Québec, QC, Canada) [15], the 2-furfuraldehyde compound (2-FAL) in Luminol was determined according to ASTM Standard D5837. The tensile index (*Tidx*) was one of the standards used to measure the inherent mechanical properties of the paper. *Tidx* was obtained by dividing the tensile strength (tensile force per paper width) by the weight (mass per square meter of paper) of the samples.

Since paper is an anisotropic and inhomogeneous material, variations in the measured tensile strength were expected. The average values were calculated. Prior to the measurement, the paper samples were de-oiled using a distilled hexane bath. Then, the papers were conditioned at an atmospheric pressure and room temperature (21 °C) inside a fume hood for at least 48 h.

The tensile strength test was assessed according to ASTM Standard D828.

The values used were for a sample 25.4 mm wide and 130 mm long, while the transverse separation speed during the test was set at 7 mm/min and the initial machine gap was 50 mm. The mechanical properties of the paper samples were measured using a tensile tester (Testing Machine Inc., series 84-76, Québec, QC, Canada).

The average inherent viscosity value based on the ASTM D4243 standard was used to calculate the DP_V of the paper samples. To determine an average value, two measurements were made on each sample.

3. Numerical Prediction Techniques

MR, PSO, and ANN techniques, which had a simple computational architecture and are widely used in the research, were best suited for the prediction.

First, a second-order polynomial was used for the MR process. The reason for choosing a polynomial of this order in this study was that several trials were conducted using different orders of polynomial regression models and the best fit was selected. The PSO optimization method was also used for its effectiveness in optimizing multiple regression models with a high number of input variables and its successful use in similar studies [10].

Finally, the ANN method based on deep learning was used. A Levenberg–Marquardt algorithm was selected for its widespread use in the research and its suitability for the database [13]. Additional details on the three methods used in the study are presented in the following flowchart: Figure 3 depicts a flowchart of the three-step process.

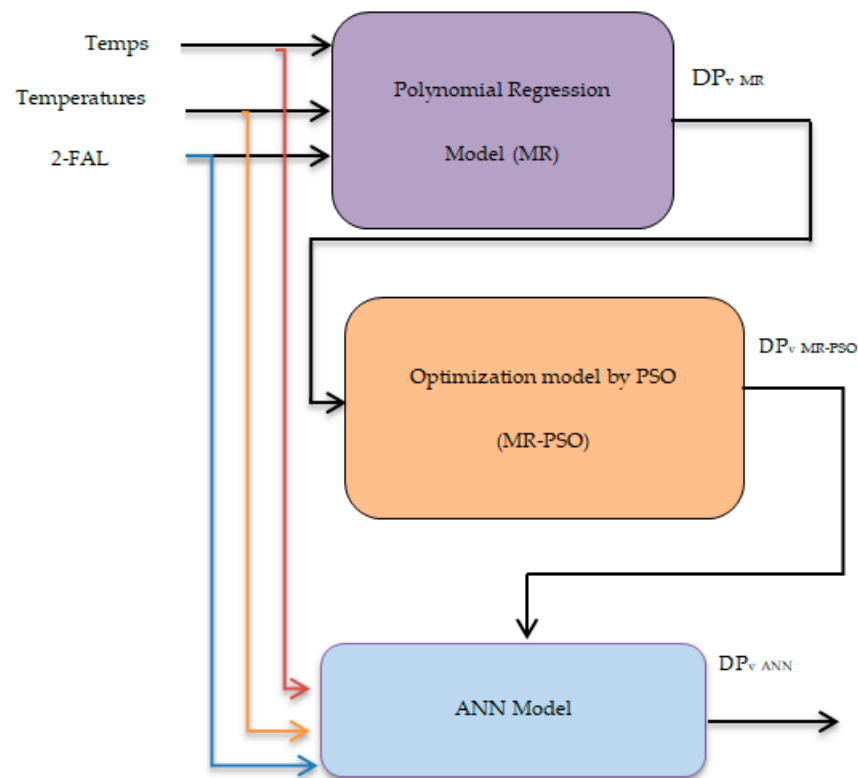


Figure 3. Flowchart of the prediction methods.

3.1. Mathematical Modeling with a Multiple Regression Model (MR)

MR is a traditional technique which is used firstly by Pearson in 1908 [16]. This technique is used to explain (or predict) the variation in a dependent interval based on linear combinations between independent intervals and Boolean or dichotomous variables. In general, the purpose of MR is to determine the relationship between several predictors or independent variables and a criterion or dependent variables.

The general format of the MR equation is given as follows:

$$\begin{aligned}
 y = & w_1 + w_2x_1 + w_3x_2 + w_4x_3 \\
 & + w_5x_1x_2 + w_6x_1x_3 + w_7x_2x_3 \\
 & + w_8x_1^2 + w_9x_2^2 + w_{10}x_3^2
 \end{aligned} \quad (1)$$

where $(w_1, w_2, w_3, \dots, w_{10})$ are the model constants that need to be determined.

In this study, the output of the model was $y = DP_V$.

The model inputs were:

- x_1 : t(h) (aging time);
- x_2 : T (°C) (aging temperature);
- x_3 : 2-FAL (ppb) (2-furfuraldehyde concentration).

The proposed model allowed predicting the mechanical properties of the insulating paper (used in power transformers subjected to thermal aging). It is important to note that models using the 2-FAL concentrations cannot be used for thermally upgraded paper (TUK), where 2-FAL is not generated at the same level in comparison to when standard kraft paper is used. This is because, in real life, the amount of 2-FAL generated depends on the number of thermal stabilizers contained in the paper. The models are therefore not applicable to a transformer built with thermally upgraded paper (TUK).

3.2. Particle Swarm Optimization (PSO) Algorithm

The PSO (a swarm algorithm) was developed by Eberhart and Kennedy, who drew their inspiration from the behavior of tiny social animals, such as fish and birds. It is one of

the metaheuristic strategies, according to [17]. The statistics community recognizes it as a developing computational method with several advantages [18,19]. The PSO approach is based on the following general principles [20]:

A swarm of size n is considered. Each swarm particle P_i , $i = 1, 2, \dots, n$ is personalized by its current position $D_i(k)$, which refers to an optimization problem solution at its iteration k , velocity $V_i(k)$, and the best position $P_{besti}(k)$ identified during its previous trajectory. $G_{besti}(k)$ is defined as the best global position found on all the trajectories traveled by the different particles of the swarm. Each of the n particle flies in the d -dimensional search area at a speed $V_i(k)$, which is dynamically adjusted according to its previous personal best solution $P_{besti}(k)$ and the previous best global solution $G_{besti}(k)$ of the whole swarm. The velocity updates are determined as a linear combination of the two positions and velocity vectors. Position, velocity, and fitness are three significant factors that are critical. The PSO is used to solve an optimization problem by performing the following [21]:

- a. Create a population of people (particles) in the issue domain with random positions and velocities;
- b. The overall fitness calculation value;
- c. Substances examining fitness;
- d. Actualization of the velocity and position of the particles using Equations (2) and (3):

$$V_i(k+1) = w(k)V_i(k) + C_1 \cdot R_1(k) \cdot (P_{besti}(k) - D_i(k)) + C_2 \cdot R_2(k) \cdot (G_{besti}(k) - D_i(k)) \quad (2)$$

$$D_i(k+1) = D_i(k) + V_i(k+1) \quad (3)$$

The acceleration constants C_1 and C_2 regulate the relative velocities with respect to the global and local best positions, respectively. The random variables R_1 and R_2 are drawn from a regular distribution in the interval $[0, 1]$, where $V_i(k+1)$ is the velocity of the $(k+1)$ th iteration of the i th individual, $V_i(k)$ is the velocity of the k th iteration of the i th individual, and $w(k)$ is the inertial weight. Low values of w produce a faster convergence, while a higher value may prevent divergence.

The PSO's advantages include simple coding and low processing cost [21]. Since the PSO algorithm solves optimal glob problems with accuracy, it is used in the current work to train the multi-layer perceptron (MLP) network models.

3.3. Artificial Neuron Networks (ANNs)

The main function of the ANN is information processing through the efficient non-linear mapping of input and output spaces. Its importance lies in its ability to learn from the implementation of a structured device of well-interconnected neurons. These artificial neurons constitute a layered network composed of two well-defined input and output layers, which can be separated by one or more hidden layers [22]. The ANN structure is properly constructed to obtain optimum accuracy with a minimum amount of complexity. However, the inputs chosen should fully define the characteristics of the problem, and thus, the output reflects the result.

In this study, MATLAB software R2015a was used to develop an ANN model which takes in consideration three main parameters such as time, temperature, and 2-FAL. The goal is to evaluate the state of the insulating paper of the transformers. The proposed model's output was DP_V .

The multilayer feed-forward-backward propagation nature of ANN models allows an easy handling of performance. These structures, which are known as universal approximators, are capable of accurately approximating any sort of continuous or nonlinear function. Through an adjustable learning rate, the Levenberg–Marquardt training algorithm, also benefits from faster training for the multilayer feed-forward architecture [23,24]. The three layers that comprise the developed ANN model are the input, hidden, and output layers, respectively (Figure 4). The NN-based models were developed and the Levenberg–Marquardt back-propagation technique was used to implement them. The output layer uses a linear

transfer function, whereas the hidden layer uses a sigmoid transfer function for training and testing purposes. The best performance for a back-propagation ANN may be seen in the highly nonlinear sigmoid activation function. The temperature range for the input parameters was adjusted from 150 to 190 °C and the aging time ranged from 0 to 5000 h.

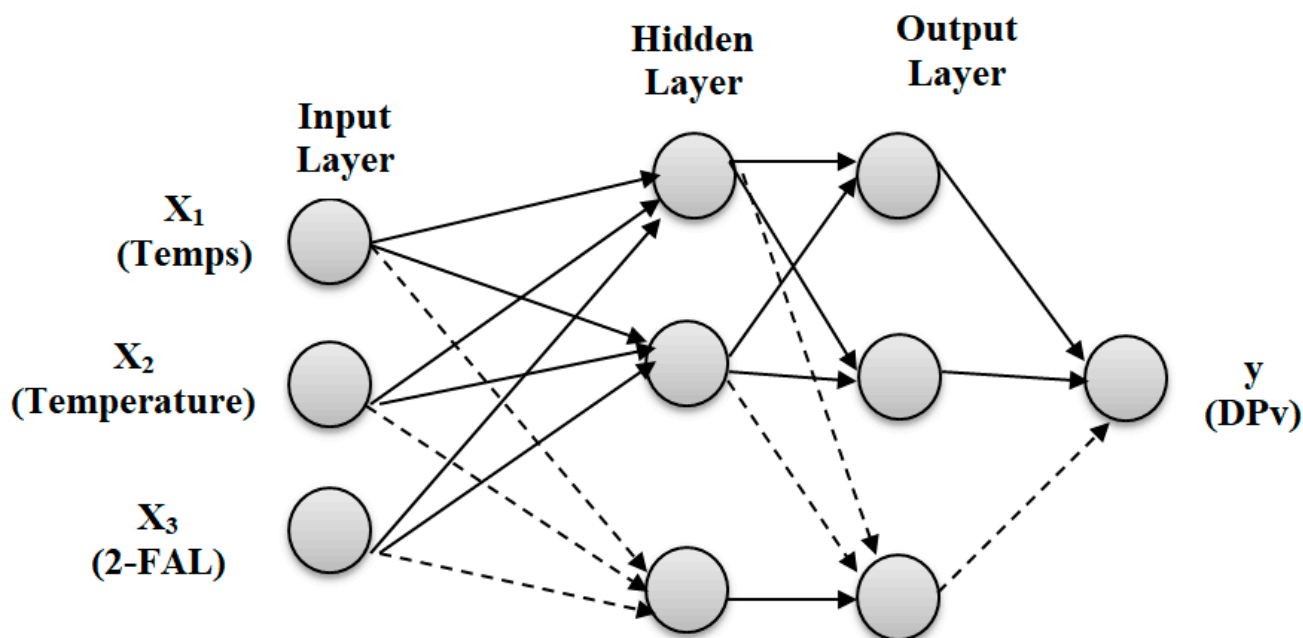


Figure 4. The concept of the MLP neural network used in this study.

An extended training dataset of 33 data points was used to train the proposed network. In order to enhance the predictability of the remaining insulation life, the hidden-layer number of neurons in the suggested insulation assessment model was modified. Using a trial strategy, it was decided that there should be 22 hidden-layer neurons, which corresponded to a minimum mean square error (*RMSE*). The least variation between the input and target values is shown by the *RMSE*. The flow diagram for stage III in Figure 5 depicts the ANN model implementation process. Table 1 provides a summary of the best settings that were used to train the integrated system's ANN model.

Table 1. Parameters of the proposed ANN model.

Specification of Proposed ANN	
Network architecture	Multilayer feed forward
Training algorithm	Levenberg–Marquardt
ANN structure	Single hidden layer in between input and output layers
Transfer function for hidden layer	Sigmoid
Transfer function for output layer	Linear
Input vector	[Time; temperature; 2-FAL]
Output vector	[DP_V]
Training data	31
Test data	31
No. of neurons	22

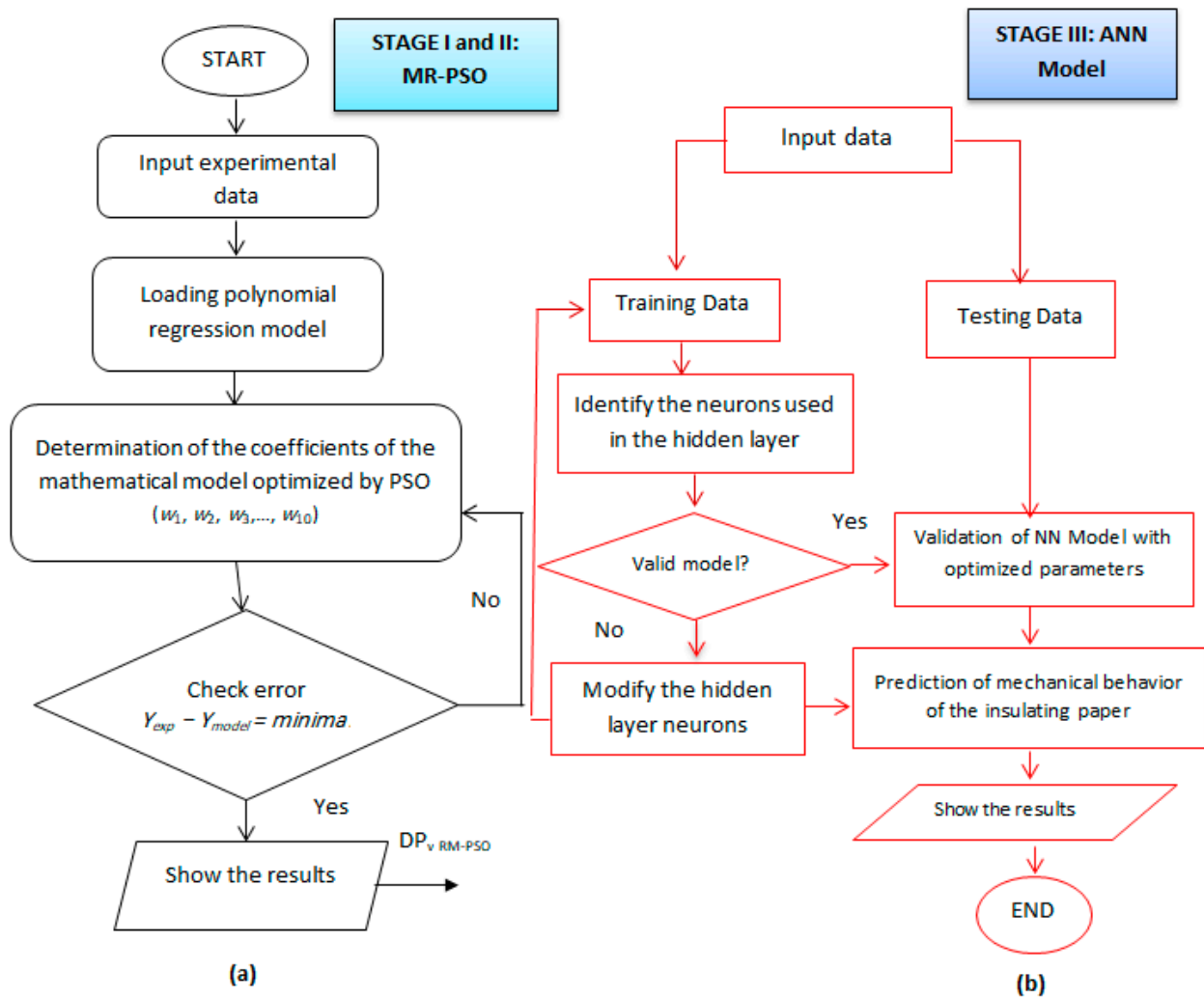


Figure 5. Flowchart of the system: (a) MR-PSO approach and (b) ANN model.

4. Modeling and Prediction of the Tensile Index

The tensile index is the common method for describing the mechanical strength of paper samples. This index is defined as the breaking force per unit length divided by the paper weight [13].

The mechanical properties of the paper were measured using a tensile tester (Testing Machine Inc., Series 84-76). The machine automatically records tensile index (*Tidx*) values. Tensile index results are expressed as a percentage change relative to the initial values for unaged paper (100%).

The tensile strength of the paper provides a relative indication of the number of warps of intact cellulose, as well as an idea of the state of the bonds between the cellulose fibers [13].

A simple regression was proposed to model the tensile index in the following format:

$$P(x) = P_1 x^n + P_2 x^{n-1} + P_3 x^{n-2} + \dots P_n x + P_{n+1} \quad (4)$$

where ($P_1, P_2, P_3, \dots, P_{13}$) are the model constants to be determined. Note that the polynomial degree n equal 12.

In this study, the output of the model was: $P = Tidx$.

The input of the model was: $x = DP_V$.

5. Evaluation Performance Indices

The root mean square error (*RMSE*) value presented in Equation (5) was calculated to evaluate the prediction performance and cost effectiveness of the prediction model developed in the study as employed by [13].

$$RMSE = \sqrt{\frac{1}{n} \sum_{i=1}^n (T_i - P_i)^2} \quad (5)$$

where P_i and T_i are the predicted and measured values, respectively.

The mean absolute percentage error (*MAPE*), which is a measure of the accuracy of a value for a statistically adjusted series, was also used to compare the predictive performance of the models. *MAPE* generally expresses the accuracy in terms of percentage (Equation (6)):

$$MAPE = \frac{1}{n} \sum_{i=1}^n \left| \frac{T_i - P_i}{T_i} \right| \times 100 \quad (6)$$

where P_i and T_i are the predicted and target values of the chosen model's property, respectively.

The regression coefficient (R^2) yields:

$$R^2 = 1 - \frac{\sum_{i=1}^n (T_i - P_i)^2}{\sum_{i=1}^n (T_i - \bar{T}_i)^2} \quad (7)$$

where T_i is the target value (the measured value of the property), P_i is the predicted value of the property by the chosen model, and \bar{T}_i is the average of the measured values.

MAE stands for the mean absolute error:

$$MAE = \frac{1}{n} \sum_{i=1}^n |T_i - P_i| \quad (8)$$

6. Results and Discussion

In this section, two main parts were highlighted. The first one focuses on the degree of polymerization (DP_V) and how accurately our model predicts changes in DP_V during aging. The second part is about the tensile index (*Tidx*) of the aged insulation paper, where the developed model is compared with actual *Tidx* values from experiments. The idea is to present a clear picture of how the paper's properties change over time and how well our model reflects this change.

6.1. Modeling and Prediction of the Degree of Polymerization (DP_V)

The experimental results reported in [13] were used as a database in the development phase of the mathematical models based on MR.

The multiple regression model developed to predict the mechanical properties of the insulating paper is of the form:

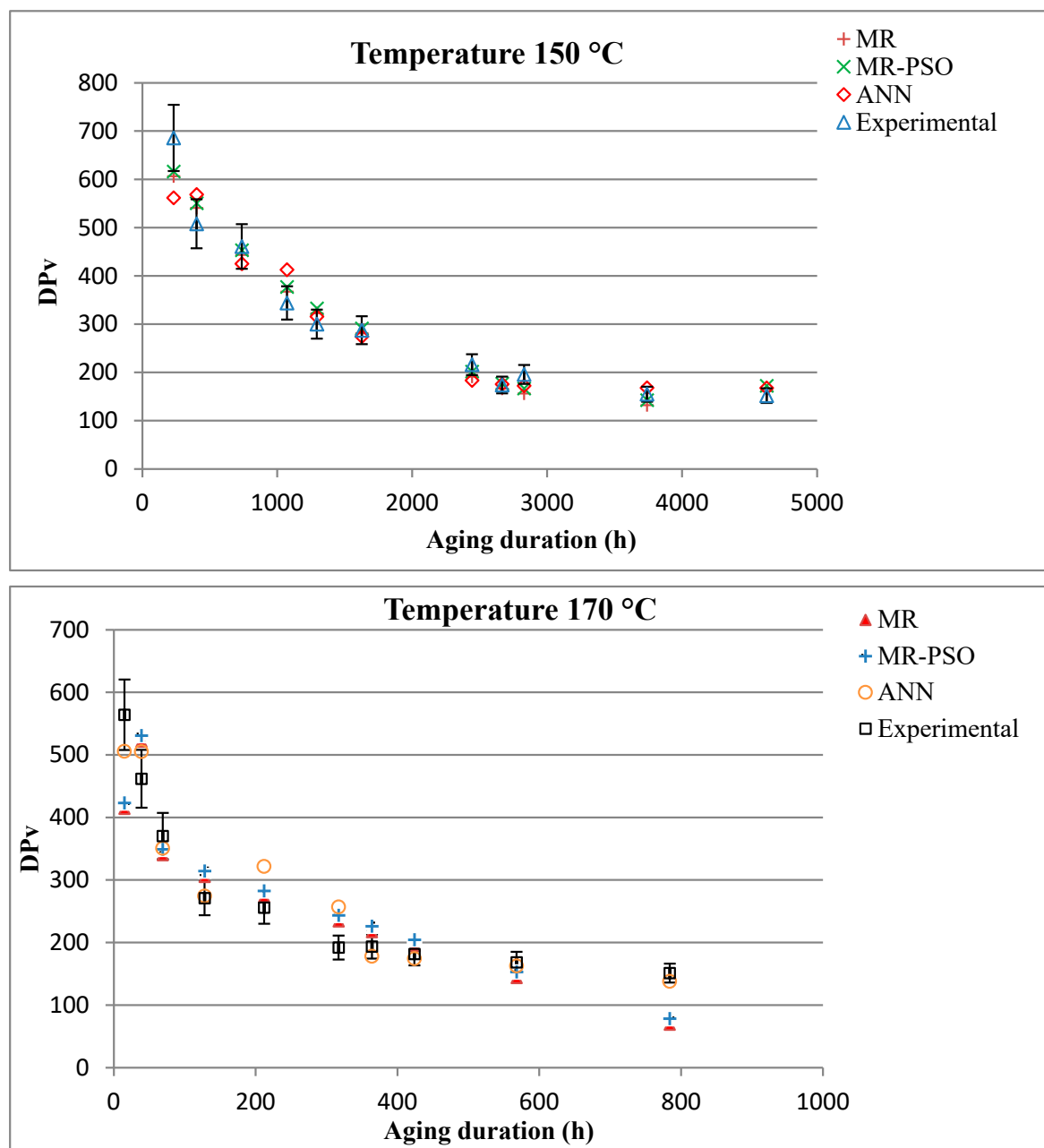
$$\begin{aligned} DP_V = & 7760.8 + 0.839 x_1 - 76.39 x_2 + 5.09 x_3 \\ & - 0.007 x_1 x_2 + 2.53 e^{-5} x_1 x_3 - 0.027 x_2 x_3 \\ & + 3.33 e^{-5} x_1^2 + 0.213 x_2^2 + 7.79 e^{-8} x_3^2 \end{aligned} \quad (9)$$

In general, the correlation factor between the measured and predicted values is a reasonable criterion for evaluating the effectiveness of the model's prediction. The simulation results are tabulated in Table 2, which indicates the performance of the model (MR), MR-PSO, and ANN models.

Table 2. Degree of polymerization indices (*RMSE*, *MAPE*, *MAE*, and R^2) for models.

Model	<i>RMSE</i>	<i>MAPE</i>	<i>MAE</i>	R^2
MR	0.4498	0.1189	0.3234	0.8955
MR-PSO	0.4498	0.1182	0.3222	0.8955
ANN	0.4244	0.1061	0.3027	0.9069

Figure 6 illustrates the prediction results of the three models (MR, MR-PSO, and ANN). The predicted results of the models are then compared to the experimental data. We can see a close agreement between the results obtained from the numerical models and the experimental data. This agreement validates the efficiency and reliability of our models in accurately capturing the behavior of the studied system.

**Figure 6.** Cont.

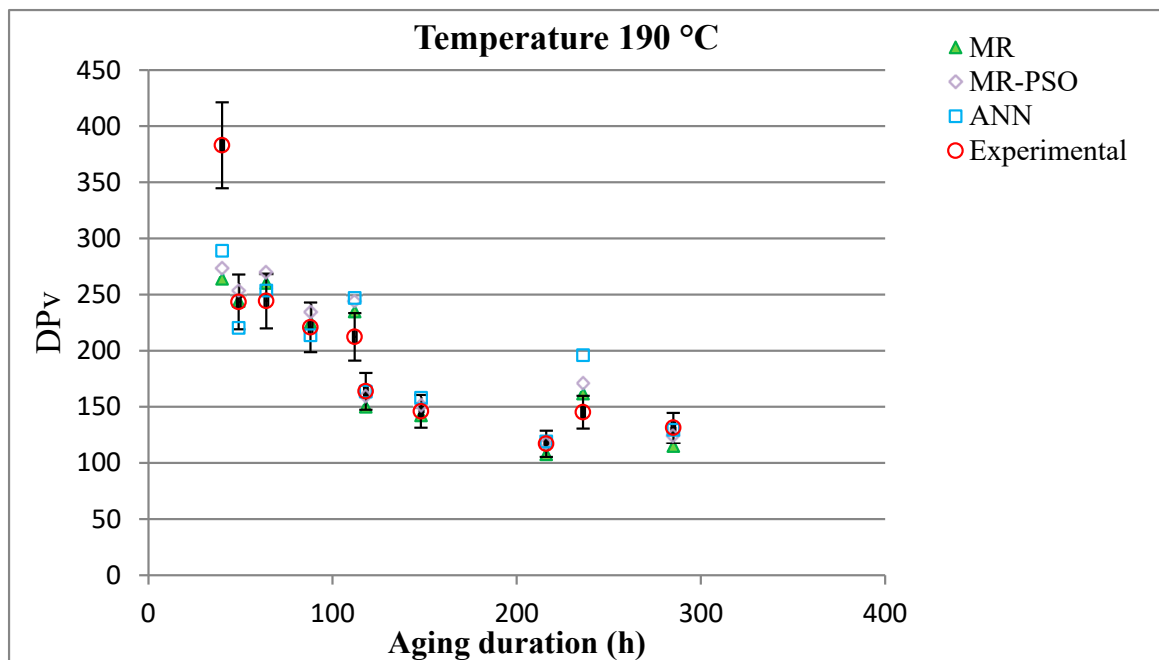


Figure 6. Experimental data along with corresponding error bars and predicted values of DP_V versus aging time at different temperatures.

The decrease in cellulose polymerization during aging shows a similar behavior, regardless of the temperature. The observed behavior indicates rapid initial depolymerization, followed by a slower decrease during the rest of the aging process. This trend suggests a single type of aging mechanism in the paper, regardless of the temperature. However, different rates of depolymerization and aging times based on the temperature were observed.

The influence of temperature on cellulose chain depolymerization was direct but non-linear, and seemed to be exponential. The results also confirm that using high temperatures for accelerated aging is acceptable.

6.2. Modeling and Prediction of the Tensile Index ($Tidx$)

The experimental results obtained from [13] were used as a database in the development phase of the mathematical models.

A simple regression model used to predict the mechanical properties of the insulating paper is presented hereafter:

$$\begin{aligned}
 Tidx(DP_V) = & -1.338e^{-26} \cdot DP_V^{12} + 6.479e^{-23} \cdot DP_V^{11} - 1.363e^{-19} \cdot DP_V^{10} \\
 & + 1.656e^{-16} \cdot DP_V^9 - 1.296e^{-13} \cdot DP_V^8 + 6.898e^{-11} \cdot DP_V^7 \\
 & - 2.569e^{-8} \cdot DP_V^6 + 6.752e^{-6} \cdot DP_V^5 - 0.001 \cdot DP_V^4 \\
 & + 0.159 \cdot DP_V^3 - 13.102 \cdot DP_V^2 + 6.36e^2 \cdot DP_V - 1.367e^4
 \end{aligned} \quad (10)$$

In general, the correlation factor between the measured and predicted values is a reasonable criterion for evaluating the good performance of the model's prediction as seen in Table 3.

Table 3. Performance of tensile index ($RMSE$, $MAPE$, MAE , and R^2) for models.

Model	$RMSE$	$MAPE$	MAE	R^2
MR	0.0546	0.1632	0.0384	0.9570
MR-PSO	0.0546	0.1630	0.0383	0.9571
ANN	0.0544	0.1629	0.03842	0.9573

The degradation of the paper's mechanical properties was assessed using the tensile index, as shown in Figure 7. The predicted results from the models were then compared to the experimental data. We observed a close agreement between the results obtained from the numerical models and the experimental data. This agreement validated the efficiency and reliability of our models in accurately capturing the behavior of the studied system.

Similar to depolymerization, two trends were observed in each curve. During the initial aging phase, there was a rapid loss of the paper's tensile strength, associated with quicker cellulose depolymerization. In the second phase, the rate of mechanical strength loss decreased slowly until the end of the aging process. At higher temperatures, the degradation of the paper's mechanical properties was quicker. Moreover, the aging temperature appeared to have an exponential effect on the degradation of the mechanical properties.

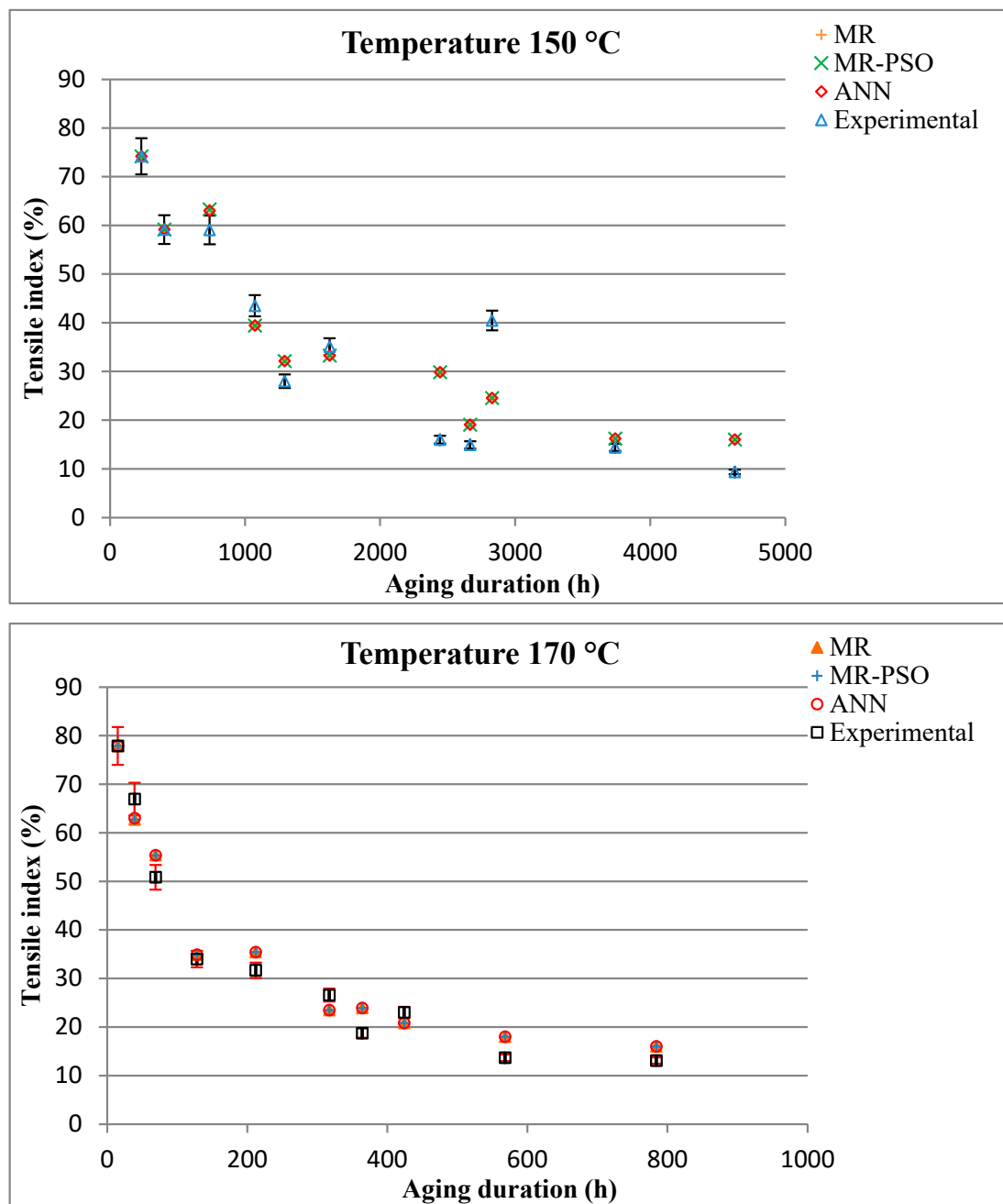


Figure 7. Cont.

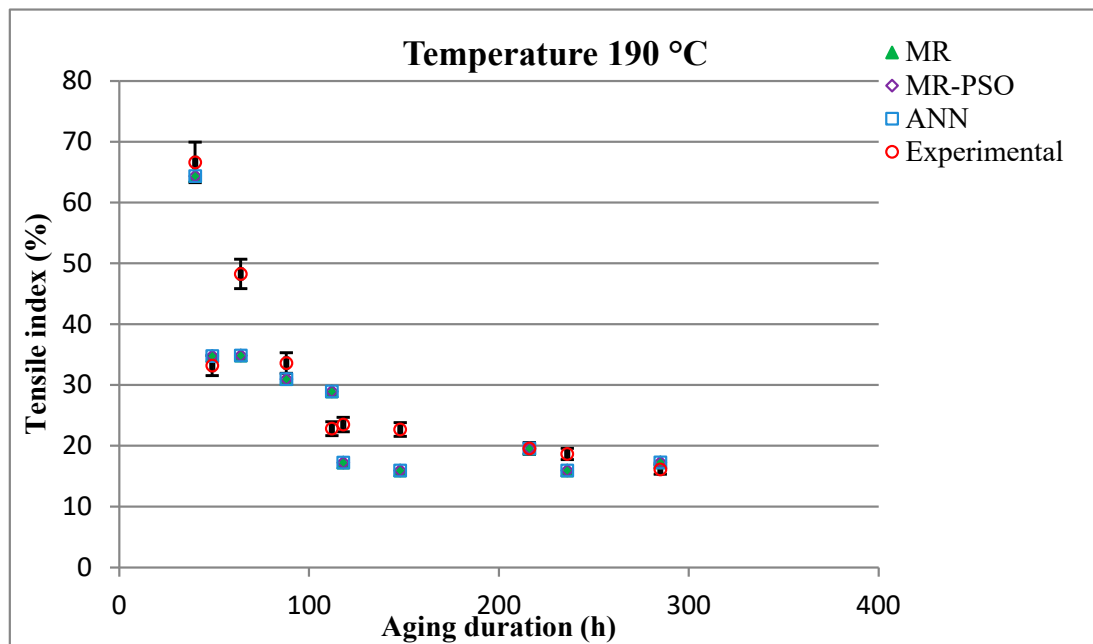


Figure 7. Experimental and predicted values of retained tensile index (%) versus elapsed aging time at different temperatures.

The comparison between the tensile index and degree of polymerization (DP_V) is illustrated in Figure 8, where the experimental results are compared with the proposed correlation curve. Overall, there is a close agreement between the experimental data and the correlation curve, particularly for temperatures of 150 and 170 °C. However, at a temperature of 190 °C, there is some deviation. This suggests that the correlation curve captures the general trend of the relationship between the tensile index and degree of polymerization; however, there might be additional factors influencing the mechanical properties at higher temperatures.

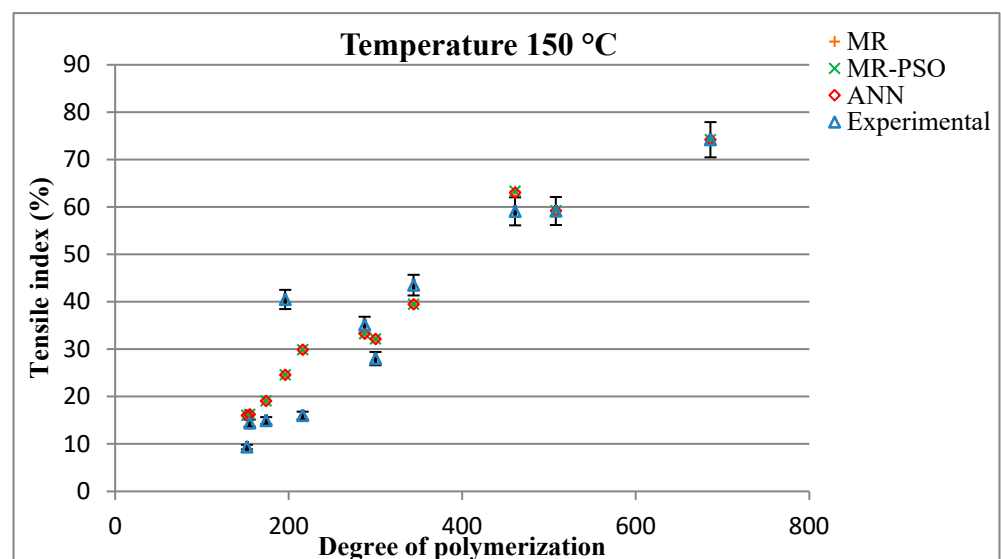


Figure 8. Cont.

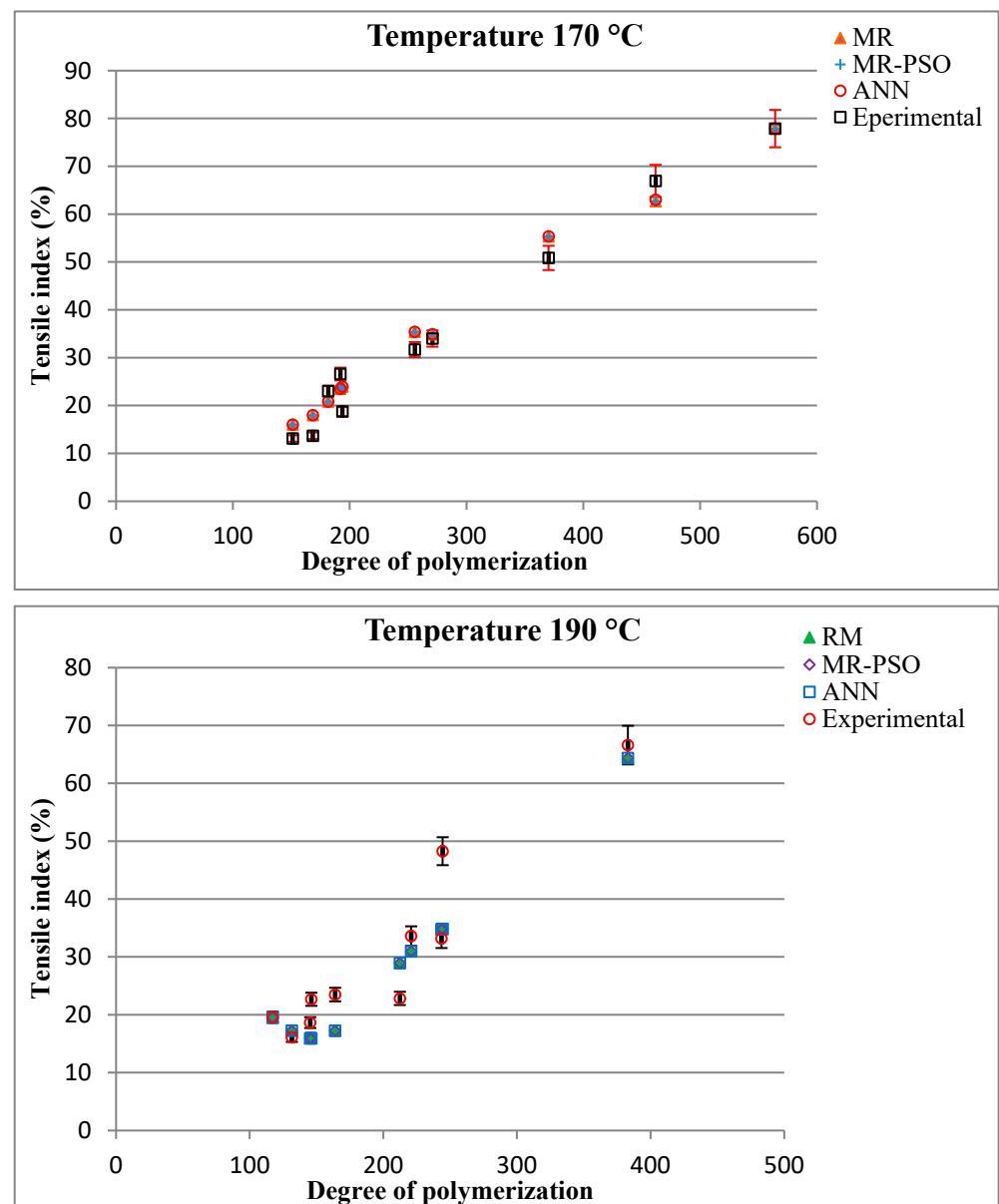


Figure 8. Correlation between the $Tidx$ (%) of papers and the DP_V .

7. Conclusions

This paper mainly focused on the use of artificial intelligence techniques to predict the behavior of the mechanical properties of standard insulating kraft paper used in power transformers under thermal aging.

The ANN technique to estimate and evaluate the behavior of the mechanical properties of the solid insulator of a transformer was developed. The proposed approach was modeled with MATLAB R2015a software.

The methodology began with the establishment of the multiple regression (MR) model using experimental datasets. The coefficients of the MR model were then optimized using the particle swarm optimization (PSO) algorithm to enhance its performance. Subsequently, the MR-PSO model was employed to train the ANN approach, capturing the nonlinear relationship between the degree of polymerization (DP_V) and the variables of time, temperature, and 2-FAL parameters.

The good performance of this model was justified by the root mean square error (RMSE), the coefficient of determination (R^2), and the mean absolute percentage error (MAPE). It can be observed that the results obtained show the effectiveness of the ap-

proaches developed based on artificial neural networks and multiple regression optimized by particle swarm optimization (PSO). From the obtained results, it can be concluded that the approaches developed in this work are able to model and predict the mechanical behavior of standard insulating kraft paper as a function of elapsed aging time.

When we analyzed at the tensile index, there was a good agreement between the experimental data and correlation curves. This validation not only affirmed the model's efficacy, but also enhanced our understanding of the aging process of insulation paper.

The utilization of artificial neural networks and multiple regression optimized by the particle swarm optimization proved to be successful in predicting the mechanical properties of insulating kraft paper under thermal aging conditions. The developed models offered valuable insights into understanding and evaluating the aging behavior of paper, which is crucial for the performance and reliability of power transformers. Future research may enhance these models further and explore additional variables to improve the accuracy of predictions and broaden their applicability.

Author Contributions: Research concept and design, A.S., D.M., I.F., J.J., O.H.A.-F. and S.A.B.; data collection and/or assembly, A.S., O.H.A.-F., S.A.B. and L.B.; data analysis and interpretation, A.S. and L.B.; writing the article, A.S., D.M., I.F. and L.B.; critical revision of the article, D.M., I.F., O.H.A.-F. and J.J.; final approval of the article, A.S., D.M., I.F., S.A.B., O.H.A.-F. and J.J. All authors have read and agreed to the published version of the manuscript.

Funding: This work was co-sponsored by the Mathematics of Information Technology and Complex Systems (MITACS) and Hydro-Québec (Grants #: IT04554, IT06653 and IT02343). This research paper is under the PRFU project n° A24N01EN030120210001, Laboratory of Applied and Didactic Sciences, Higher Normal School of Laghouat.

Data Availability Statement: Not applicable.

Acknowledgments: Ahmed Sayadi is thankful to I. Fofana, holder of the research chair on the aging of power network infrastructure (ViAHT) at the University of Québec at Chicoutimi (Canada), for the fruitful advice and permanent orientation. He is also thankful to his supervisor D. Mahi for the continuous support. Thanks are also extended to M.M.B. Benyammi, W. Bessas, and H. Rayane (students at the University of Laghouat, Algeria) for their help throughout the realization of this work.

Conflicts of Interest: The authors declare no conflict of interest.

Appendix A

Observation: $Tidx$ up to 127 J/g and DP_V up to 1500 (time = 0 (h)) for kraft paper.

Table A1. Experimental values at T = 150 °C [13]. Kraft/Luminol oil –150° C.

Time (h)	DP_V	DP_V SD	2-FAL	$Tidx$ (%) (Tensile Index)	$Tidx$ SD (%)
232	686.1	68.61	72	74.2	3.8
402	507.9	50.79	46	59.2	3.2
737	461.0	46.10	20	59.1	0.9
1072	344.0	34.40	7	43.5	4.0
1293	300.1	30.0.1	<MDL	28.0	3.2
1626	287.5	28.75	7	35.1	3.7
2443	216.1	21.61	7	16.0	1.6
2666	174.0	17.40	<MDL	14.9	1.7
2829	196.0	19.60	<MDL	40.5	2.7
3740	155.0	15.50	<MDL	14.4	1.4
4626	151.8	15.18	<MDL	9.4	1.6

Table A2. Experimental values at T = 170 °C [13]. Kraft/Luminol oil –170° C.

Time (h)	DP _V	DP _V SD	2-FAL	Tidx (%) (Tensile Index)	Tidx SD (%)
15	564.2	56.42	124	77.9	3.3
39	461.9	46.19	345	67.0	4.0
69	370.3	37.03	23	50.9	3.5
128	270.9	27.09	<MDL	34.0	1.7
212	255.7	25.57	<MDL	31.7	7.0
317	192.0	19.20	<MDL	26.6	4.1
364	193.7	19.37	<MDL	18.8	2.7
424	181.6	18.16	<MDL	23.0	1.5
568	168.4	16.84	<MDL	13.7	2.3
784	151.2	15.12	<MDL	13.1	3.8

Table A3. Experimental values at T = 190 °C [13]. Kraft/Luminol oil –190° C.

Time (h)	DP _V	DP _V SD	2-FAL	Tidx (%) (Tensile Index)	Tidx SD (%)
40	383.1	38.31	985	66.6	2.6
49	243.5	24.35	2743	33.2	2.2
64	244.4	24.44	<MDL	48.3	2.4
88	220.8	22.08	2936	33.6	2.2
112	212.4	21.24	<MDL	22.8	4.6
118	163.9	16.39	13079	23.5	1.1
148	146.1	14.61	13483	22.7	1.8
216	117.1	11.71	27345	19.6	1.7
236	145.3	14.53	1984	18.7	1.6
285	131.5	13.15	18747	16.1	5.2

References

1. Fofana, I. 50 years in the development of insulating liquids. *IEEE Electr. Insul. Mag.* **2013**, *29*, 13–25. [\[CrossRef\]](#)
2. Shroff, D.H.; Stannett, A.W. A review of paper aging in power transformers. *IEE Proc. C-Gener. Transm. Distrib.* **1985**, *132*, 312–319. [\[CrossRef\]](#)
3. Miyagi, K.; Oe, E.; Yamagata, N. Evaluation of Aging for Thermally Upgraded Paper in Mineral Oil. *J. Int. Counc. Electr. Eng.* **2011**, *1*, 181–187. [\[CrossRef\]](#)
4. Senoussaoui, M.A.; Brahami, M.; Fofana, I. Combining and comparing different machine learning algorithms to improve dissolved gas analysis interpretation. *IET Gener. Transm. Distrib.* **2018**, *12*, 3673–3679. [\[CrossRef\]](#)
5. Kusan, H.; Aytakin, O.; O' Zdemir, I. The use of fuzzy logic in predicting house selling price. *Expert. Syst. Appl.* **2010**, *37*, 1808–1813. [\[CrossRef\]](#)
6. Boukezzi, L.; Boubakeur, A. Prediction of mechanical properties of XLPE cable insulation under thermal aging: Neural network approach. *IEEE Trans. Dielectr. Electr. Insul.* **2013**, *20*, 2125–2134. [\[CrossRef\]](#)
7. Sudheer, K.; Veeranna, V. To predict mechanical properties of XLPE insulation cables under thermal ageing using neural networks and fuzzy logic techniques. *Int. J. Eng. Res. Appl.* **2022**, *12*, 5–19.
8. Ge, X.; Given, M.; Stewart, B.G. Determining accelerated aging power cable spatial temperature profiles using Artificial Neural Networks. In Proceedings of the 2022 IEEE International Conference on High Voltage Engineering and Applications (ICHVE), Chongqing, China, 25–29 September 2022.
9. Boukezzi, L.; Boubakeur, A. Comparison of some neural network algorithms used in prediction of XLPE HV insulation properties under thermal aging. In Proceedings of the 2012 IEEE International Conference on Condition Monitoring and Diagnosis, Bali, Indonesia, 23–27 September 2012. [\[CrossRef\]](#)
10. Rao, U.M.; Sood, Y.R.; Jarial, R.K. Oxidation stability enhancement of a blend of mineral and synthetic ester oils. *IEEE Electr. Insul. Mag.* **2016**, *32*, 43–47. [\[CrossRef\]](#)
11. Sayadi, A.; Mahi, D.; Bessissa, L.; Benyammi, B. Predictive modeling of the dielectric of a power transformer. In Proceedings of the 3rd National Conference on Applied Physics & Chemistry (NCAPC 2023), Laghouat, Algeria, 12–13 March 2023.

12. Abdi, S.; Haddad, A.M.; Harid, N.; Boubakeur, A. Modelling the Effect of Thermal Aging on Transformer Oil Electrical Characteristics Using a Regression Approach. *Energies* **2023**, *16*, 381. [[CrossRef](#)]
13. Arroyo, O.H. Étude des Corrélations Entre les Propriétés Mécaniques des Papiers et les Traceurs Chimiques Issus de Son Vieillessement Pour Surveiller l'état de L'isolation Solide des Transformateurs de Puissance. Thèse de Doctorat D'université, Université du Québec à Chicoutimi, Québec, QC, Canada, 2017.
14. Arroyo, O.H.; Jalbert, J.; Fofana, I.; Ryadi, M. Temperature dependence of methanol and the tensile strength of insulation paper: Kinetics of the changes of mechanical properties during ageing. *Cellulose* **2017**, *24*, 1031–1039. [[CrossRef](#)]
15. Ghoneim, S.S.M. The Degree of Polymerization in a Prediction Model of Insulating Paper and the Remaining Life of Power Transformers. *Energies* **2021**, *14*, 670. [[CrossRef](#)]
16. Yilmaz, I.; Kaynar, O. Multiple regression, ANN (RBF, MLP) and ANFIS models for prediction of swell potential of clayey soils. *Expert Syst. Appl.* **2011**, *38*, 5958–5966. [[CrossRef](#)]
17. Eberhart, R.; Kennedy, J. A new optimizer using particle swarm theory. MHS'95. In Proceedings of the Sixth International Symposium on Micro Machine and Human Science, Nagoya, Japan, 4–6 October 1995; pp. 39–43. [[CrossRef](#)]
18. Nguyen, H.; Moayedi, H.; Foong, L.K.; Al Najjar, H.A.H.; Jusoh, W.A.W.; Rashi, A.S.A.; Jamali, J. Optimizing ANN models with PSO for predicting short building seismic response. *Eng. Comput.* **2020**, *36*, 823–837. [[CrossRef](#)]
19. Yang, X.; Zhang, Y.; Yang, Y.; Lv, W. Deterministic and Probabilistic Wind Power Forecasting Based on Bi-Level Convolutional Neural Network and Particle Swarm Optimization. *Appl. Sci.* **2019**, *9*, 1794. [[CrossRef](#)]
20. Kennedy, J.; Eberhart, R. Particle swarm optimisation. In Proceedings of the 1995 IEEE International Conference on Neural Network, Perth, WA, Australia, 27 November–1 December 1995; pp. 1942–1948.
21. Belkebir, A.; Bourek, Y.; Benguesmia, H. Particle swarm optimization of a neural network model for predicting the flashover voltage on polluted cap and pin insulator. *Diagnostyka* **2022**, *23*, 2022309. [[CrossRef](#)]
22. Equbal, M.D.; Khan, S.A.; Islam, T. Transformer incipient fault diagnosis on the basis of energy-weighted DGA using an artificial neural network. *Turk. J. Electr. Eng. Comput. Sci.* **2018**, *26*, 77–88. [[CrossRef](#)]
23. Thango, B.A.; Bokoro, P.N. Prediction of the Degree of Polymerization in Transformer Cellulose Insulation Using the Feedforward Backpropagation Artificial Neural Network. *Energies* **2022**, *15*, 4209. [[CrossRef](#)]
24. Chaturvedi, D.K.; Satsangi, P.S.; Kalra, P.K. Flexible neural network models for electrical machine. *J. Inst. Eng.* **1999**, *80*, 53–58.

Disclaimer/Publisher's Note: The statements, opinions and data contained in all publications are solely those of the individual author(s) and contributor(s) and not of MDPI and/or the editor(s). MDPI and/or the editor(s) disclaim responsibility for any injury to people or property resulting from any ideas, methods, instructions or products referred to in the content.